Finite-length charge-density waves on terminated atomic wires

Jin Sung Shin,[1,2] Kyung-Deuk Ryang,[2] and Han Woong Yeom[1,3,*]

[1]*Center for Atomic Wires and Layers, Pohang University of Science and Technology, Pohang 790-784, Korea*
[2]*Department of Physics, Yonsei University, Seoul 120-749, Korea*
[3]*Department of Physics, Pohang University of Science and Technology, Pohang 790-784, Korea*

Finite-size effects in charge-density waves (CDWs) were unveiled using scanning tunneling microscopy for metallic atomic wires on the Au/Si(553) surface, as terminated by adsorbate impurities. We found that CDW formed at low temperature adopts the finite-length boundary condition in two distinct ways, depending on the length scale. For longer wires than $\sim$10 nm, the CDW correlation length, the decay length of the CDW amplitude from the terminating ends, scales continuously with the wire length as predicted in a recent hyperscaling theory [Phys. Rev. B **75**, 205428 (2007)]. For shorter wires, the boundary condition becomes discrete with respect to the CDW wavelength of $3a_0$. For incommensurate wire lengths with $3a_0$, fluctuating CDW states were observed, which are due to the motion of solitonlike antiphase boundaries.

Finite-size effects[1] provide challenging issues and opportunities in condensed matter physics, since quantum states of matter are largely affected or controlled by the size of the systems or domains. For example, the superconducting correlation in thin metal films scales with the film thickness,[2] and the ferromagnetic ordering depends on the size of the magnetic particles and wires.[3] However, there are quite a few interesting and important quantum states of matter for which the finite-size effect has not been fully disclosed. This is often due to the limitation in the systematic size control for a given material system.

Charge-density wave (CDW) is an important quantum state for low-dimensional electron systems,[4] for which the finite-size effect has not been detailed to the best of our knowledge. Ideally, CDW occurs in one-dimensional (1D) metals through the electron-phonon interaction and is characterized with a single particle gap and periodic spatial modulations of the charge density and the lattice.[4,5] Any study of the finite-size effect for CDW requests 1D metals with controllable lengths, which have been hard to realize. On the other hand, a very recent theoretical study suggested that the CDW correlation scales with the length of the finite-size 1D system,[6] which requires experimental verification.

As exploited here, a new type of 1D metals, self-assembled metallic atomic wires on semiconductor surfaces, provides further controllability over conventional bulk 1D materials. In particular, vicinal silicon surfaces such as Si(553) were found to accommodate well-ordered atomic wire arrays when reacted with submonolayer gold atoms [see Fig. 1(a)]. The wire array on Si(553) exhibits a 1D metallic band structure[7–11] and a phase transition into a CDW state at low temperature with a tripled period ($3a_0$ with $a_0 = 0.384$ nm, the size of the silicon surface unit cell).[8–16]

One particular aspect of this system we noted is that water adsorbates interact strongly with the wires and make vacancy-type defects to terminate the wires into finite-length rods [see Figs. 1(a) and 1(b)].[17,18] The electronic state near the Fermi level, related to the CDW state, was shown to be confined within the finite-length rods.[19] Since the density of water adsorbates is easily controlled, one can access 1D

metallic rods for a full span of the length from the atomic scale.

In this paper we examined the CDW state at low temperature in detail using scanning tunneling microscopy (STM) along those terminated atomic wires with various lengths from one to a few tens of nanometers. For relatively long wires we found the CDW correlation length to scale with the total length of the wire, verifying the recent hyperscaling theory which extended the scaling property of the CDW order into the system size.[6] For short wires (rods), a discrete length dependence is observed with respect to the CDW wavelength of $3a_0$. That is, there exist commensurate and incommensurate lengths of $3na_0$ and $(3n + 1)a_0$ or $(3n + 2)a_0$ (n, an integer), respectively, which show distinct CDW states. The fluctuating CDW state observed for the incommensurate length rods is attributed to the motion of the solitonlike antiphase boundaries.

The experiments were performed using a commercial variable-temperature STM system (Omicron, Germany) operating at 40–300 K. The clean Si(553) surfaces were prepared by flash heating to 1500 K with a current parallel to step edges.[20] The well-ordered atomic wire array was prepared by the deposition of $\sim$0.5 monolayer Au onto the sample at 920 K.[8,11,17,21]

Figure 1(a) shows the empty-state STM image of Au/Si(553) at room temperature (RT). Above the CDW transition temperature ($T_c \sim 250$ K), the surface structure exhibits a period of a_0 along the wire and $4\frac{1}{3}a_0$ (1.48 nm) between the wires. The atomic structure, for which the most recent model is shown in Fig. 1(g),[22] is still under debate, but most of the models agree that the alternating bright and dark chains correspond to rows of Si step-edge atoms and Au atoms substituted into the top Si layer of terraces, respectively.[9,22–26] In this work we focus on the most prominent feature, the bright chains of step-edge Si atoms.

Figures 1(a) and 1(b) show a few vacancylike defects on the step-edge chains which have an identical structure with a length of $2a_0$ (or $5a_0$ from one end of the normal chain to the other end) [see Fig. 1(e)].[18,19] These defects are due to dissociated water adsorbates from the residual gas.[18] The defect density is thus determined by the water partial pressure
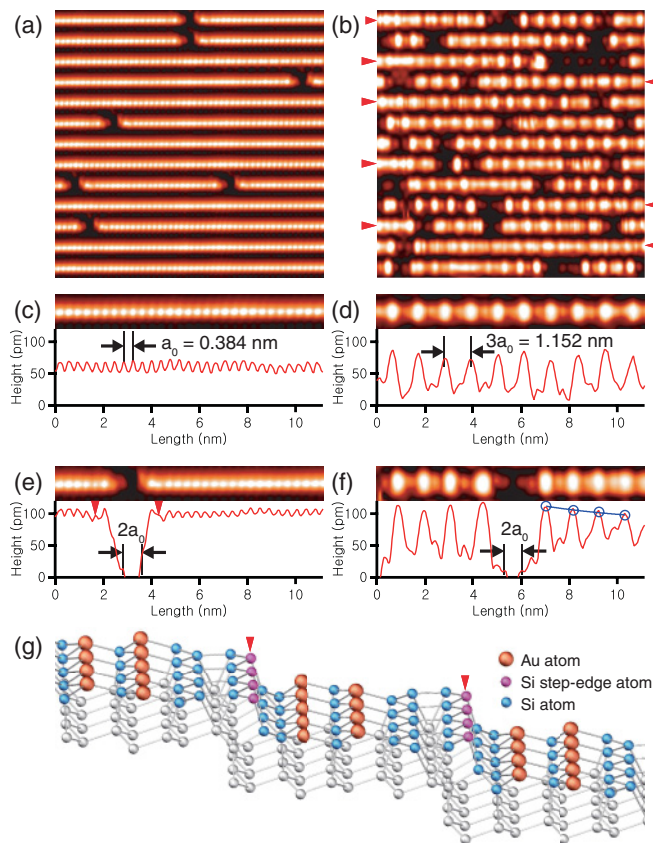
FIG. 1. (Color online) (a) and (b) 19.2×19.2 nm STM topographies above (RT) and below (87 K) the CDW transition temperature, respectively. a_0 and $3a_0$ structures along the step-edge atomic chains, bright protrusions, are clear in (a) and (b), respectively. Sample bias is $+1.0$ V, and tunneling current is 50 pA. (c) and (d) [(e) and (f)] The STM images and the corresponding line profiles of the step-edge chains at RT and 87 K, respectively, without (with) an adsorbate defect. (g) One of the proposed structure models, which features two Au atomic chains incorporated onto each terrace and the step-edge Si chains (indicated by arrowheads), appearing as bright chains in the STM images.[22]

and can be increased intentionally by introducing the water vapor.[18] It was demonstrated that these defects confine the electronic states near the Fermi level for very short wires at RT.[19] This must be related to the large local band gap on the defect.[18] Another important point is that the structural distortion in the vicinity of a defect is fairly marginal and well localized; only up to three unit cells are apparently affected, as indicated by arrowheads in Fig. 1(e). This is important for studying the CDW state around a defect without an extended structural perturbation.

Below T_c, a huge modulation emerges at the step-edge chains with a period of $3a_0$ as shown in Figs. 1(b) and 1(d). This modulation is out of phase between empty and filled states, indicating the charge ordering.[16] Its CDW origin was further supported by (i) the well-nested Fermi surface in the RT phase, with a nesting vector consistent with the CDW wavelength, and (ii) the band-gap opening for the modulated phase.[11] However, even well below T_c, one can notice substantial inhomogeneity in the CDW order. While other parts of the wires exhibit a clear $3a_0$ CDW modulation, the chains indicated by arrowheads in

Fig. 1(b) show irregular modulations with ill-defined periods and varying amplitudes. As illustrated in Fig. 1(f), even for an isolated defect, the left and right parts often exhibit distinct CDW orders. This does not fit with the idea that the irregularity may be caused by and propagates from a single defect. No sign of the interwire coupling or the coupling with a defect in neighboring wires was noticed.

As unveiled below, these irregularities are mostly due to different boundary conditions imposed by two neighboring defects. The CDW states are thus analyzed systematically as a function of the wire length defined by two defects. We first start with the case of relatively long wires ($10 \sim 60$ nm) (see Fig. 2). For these long wires, the CDW amplitude is maximized at the ends and decays away toward the center of the wire. This indicates that the CDW amplitude and phase is well pinned at the terminating ends of wires and the CDW has finite correlation lengths. What is intriguing is that this decay depends on the length of the wires. In order to quantify the decay, we define the CDW amplitude (open circles in Fig. 2) as the height difference between one CDW maximum and its neighboring minimum. The CDW amplitude was then fit with an exponential decay function of $A \exp(-L/\tau)$ (solid lines). The inset of Fig. 2 collects the decay lengths τ obtained from a few long wires. This clearly shows that the CDW decay length increases as the wire length extends. The increase observed is as large as 900% for the length range sampled. This cannot be understood as the local effect of a single defect that would give a constant decay length irrespective of the distance from the neighboring defects or the length of the wire. In this case, one cannot simply define a global correlation length as defined by the temperature and the defect density.

For the finite-size effect on CDW, we could find one very recent theoretical study in the literature.[6] According to this theory, the CDW correlation length at a fixed temperature is governed by the ratio of the chain length to the critical length L_c determined by the Fermi wave vector and the CDW energy gap. When $L > L_c$, the CDW order is fully developed as in the infinite-length case. However, the CDW correlation decays from the wire ends for $L \lesssim L_c$, where τ decreases as the wire length decreases. That is, for a finite system, the size of the system acts as a scaling parameter on the CDW order in a similar way to the temperature; a smaller size resembles a higher temperature. This is fully consistent with the present observation. For the present system, L_c is estimated as ~ 20 nm from the band dispersion measurement.[11] This value only qualitatively agrees with the observed length scale here, where L_c is estimated to be larger than 60 nm. The rather large quantitative difference between the theory and the experiment may be due to the approximation method used in the theory, especially the exclusion of the lattice effect, strong in the present case of a commensurate CDW, and the finite interwire coupling, both of which would extend the CDW correlation length substantially.

The theoretical approach using a continuous medium without a lattice cannot give insights into the CDW behavior for very short wires where the discrete lattice effect cannot be neglected.[6] This is the case for short chains of lengths between $12a_0$ and $23a_0$, shown in Fig. 3. The CDW modulations in these wires do not simply depend on the length but are categorized by the relationship between the length and the CDW wavelength,
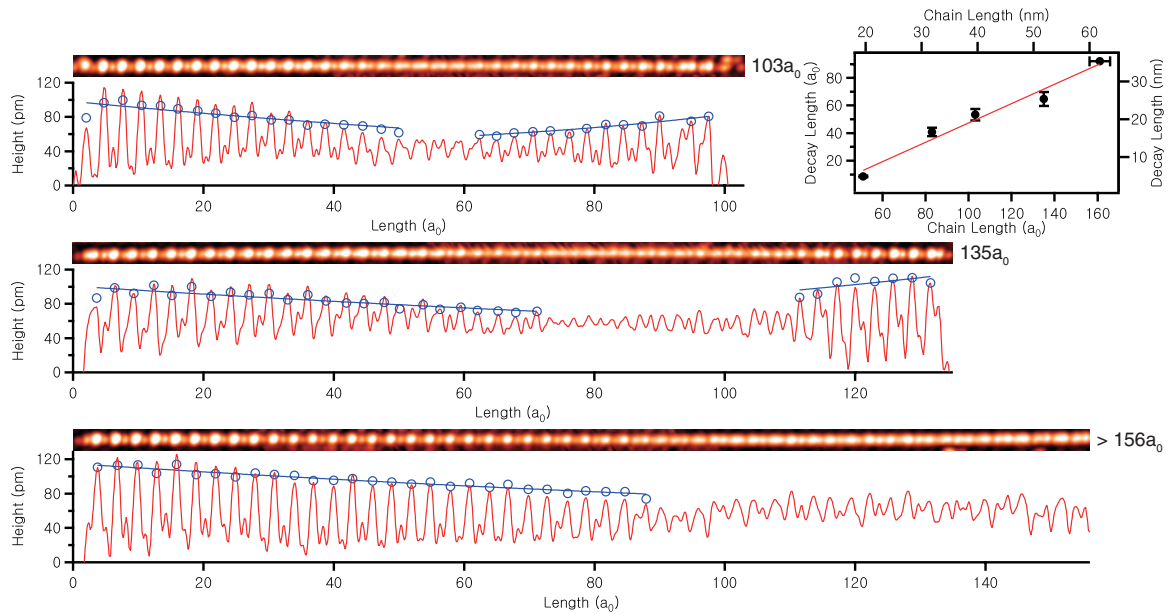
FIG. 2. (Color online) STM images at the same scanning conditions as Fig. 1 and corresponding line profiles of long chains at 47 K. The open circles indicate the CDW amplitude as defined in the text and solid lines the exponential fits for them. The inset shows the relation between the length of wires and the decay length of the CDW amplitude obtained from these fits.

that is, $3na_0$, $(3n + 1)a_0$, and $(3n + 2)a_0$. In the *commensurate* case of $3na_0$, the CDW wavelength fits well with the boundary condition and the wires have a well-ordered $3a_0$-period CDW with a uniform amplitude. In other words, the phases of the CDWs pinned by the two ends match well. But in the other two *incommensurate* cases, a clear $3na_0$ modulation is not observed but rather irregular ones were observed. This irregularity is more substantial for the $(3n + 2)a_0$ cases. We further found that these irregular modulations are not static but fluctuating in a time scale faster than the scanning speed of 0.1–0.3 nm/s.[27]

When the surface is cooled further to 47 K, we observed more static modulations as shown in Figs. 3(d) and 3(e). At this temperature, one can identify roughly the $3na_0$ CDW but with local misfits of the length $4a_0$ for $(3n + 1)a_0$ wires [Fig. 3(e)] and $2a_0$ for $(3n + 2)a_0$ [Fig. 3(d)]. These misfits are antiphase boundaries, where the phase of CDW is shifted by $2\pi/3$ or $4\pi/3$, respectively, between CDWs pinned at opposite ends of a wire. These misfits are found for most of the wires sampled at 47 K, about 20 different wires, with incommensurate lengths of $(3n + 1)a_0$ and $(3n + 2)a_0$. As shown in the supporting information,[27] the CDW line profiles of snapshot images at
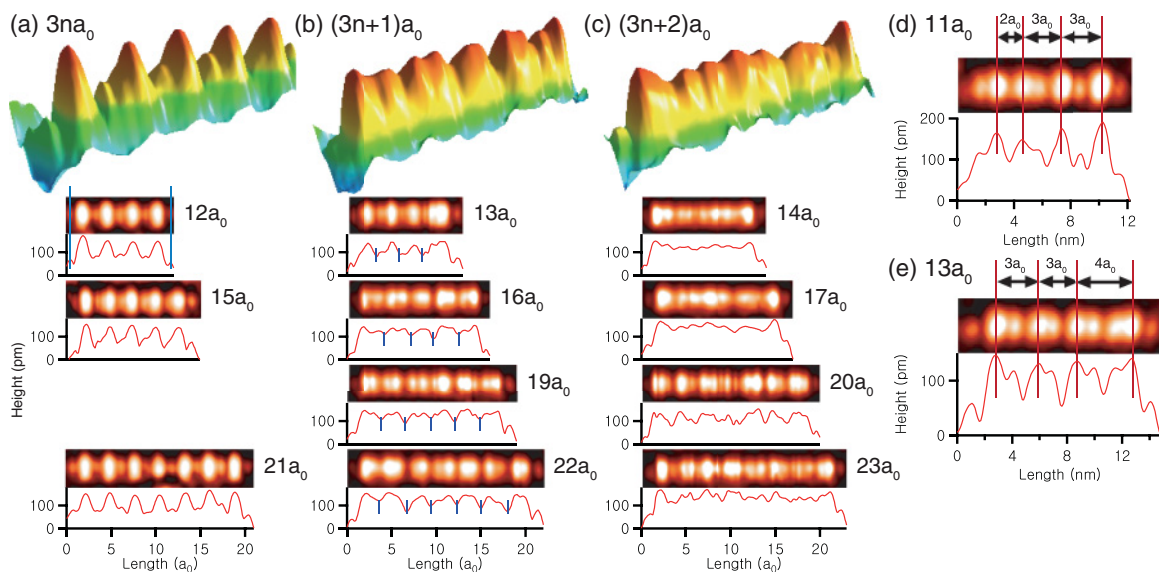

FIG. 3. (Color online) STM images in two- and three-dimensional plots at the same scanning conditions as Fig. 1 and corresponding line profiles for the short chains with lengths of (a) $15a_0$, (b) $16a_0$, and (c) $17a_0$ at 87 K. The two-dimensional STM images and line profiles for the chains of other lengths are also shown for comparison. Similar data at 47 K for the wires of lengths (d) $11a_0$ and (e) $12a_0$, which contain $2a_0$ and $4a_0$ antiphase boundaries, respectively.

a higher temperature of 87 K can largely be explained by two CDWs pinned at both ends. That is, the incommensurate lengths for these wires are compensated by creating antiphase misfit boundaries and the irregular fluctuations can be largely due to the motion of these boundaries. In principle, an antiphase boundary in a CDW state can largely be treated as a soliton excitation. It is very interesting that this system features two different types of boundaries with different structures as naturally and theoretically predicted for solitons in a $3a_0$ CDW system.[28] A detailed investigation on the soliton properties of these antiphase boundaries is left for a forthcoming work.

In summary, we disclosed the finite-length effect on 1D CDW for the first time. The $3a_0$-period CDW state of the atomic wires on the Au/Si(553) surface was investigated using STM, where the finite-length CDW wires are formed by random adsorbate defects. Finite-length CDW exhibits distinct behaviors with respect to the length scale. For long wires (10 ∼ 60 nm), the CDW correlation increases as the wire length increases, as predicted in a recent theory. For short wires ($\lesssim$10 nm), discrete boundary conditions with respect to the CDW wavelength were observed; while a well-defined CDW is observed for a commensurate length of $3na_0$, the wires with incommensurate lengths exhibit irregular fluctuation patterns. The fluctuation originates from the motion of antiphase boundaries created by the pinning of the CDW phases at both terminating defects. This demonstrates clearly how the finite-size effect itself changes drastically when the size shrinks below 10 nm, becoming comparable to the characteristic length scale of a given quantum state. This new type of nanosystem, self-assembled atomic wires terminated by adsorbates, provides the possibility to directly and easily access the intriguing 1D physics with finite and widely varied lengths.

[*]yeom@postech.ac.kr

[1]*Finite Size Scaling and Numerical Simulation of Statistical Systems*, edited by V. Privman (World Scientific, Singapore, 1990), and references herein.

[2]C. Brun, I.-P. Hong, F. Patthey, I. Y. Sklyadneva, R. Heid, P. M. Echenique, K. P. Bohnen, E. V. Chulkov, and W.-D. Schneider, Phys. Rev. Lett. **102**, 207002 (2009), and references herein.

[3]D. Weller and A. Moser, IEEE Trans. Magn. **35**, 4423 (1999); K.-J. Kim, J.-C. Lee, S.-M. Ahn, K.-S. Lee, C.-W. Lee, Y. J. Cho, S. Seo, K.-H. Shin, S.-B. Choe, and H.-W. Lee, Nature (London) **458**, 740 (2009).

[4]R. E. Peierls, *Quantum Theory of Solids* (Oxford University Press, London, 1956).

[5]G. Grüner, *Density Waves in Solids* (Addison-Wesley, Reading, MA, 1994).

[6]D. F. Urban, C. A. Stafford, and H. Grabert, Phys. Rev. B **75**, 205428 (2007).

[7]H. W. Yeom, S. Takeda, E. Rotenberg, I. Matsuda, K. Horikoshi, J. Schaefer, C. M. Lee, S. D. Kevan, T. Ohta, T. Nagao, and S. Hasegawa, Phys. Rev. Lett. **82**, 4898 (1999).

[8]J. N. Crain, A. Kirakosian, K. N. Altmann, C. Bromberger, S. C. Erwin, J. L. McChesney, J.-L. Lin, and F. J. Himpsel, Phys. Rev. Lett. **90**, 176805 (2003).

[9]J. N. Crain, J. L. McChesney, F. Zheng, M. C. Gallagher, P. C. Snijders, M. Bissen, C. Gundelach, S. C. Erwin, and F. J. Himpsel, Phys. Rev. B **69**, 125401 (2004).

[10]J. R. Ahn, H. W. Yeom, H. S. Yoon, and I.-W. Lyo, Phys. Rev. Lett. **91**, 196403 (2003).

[11]J. R. Ahn, P. G. Kang, K. D. Ryang, and H. W. Yeom, Phys. Rev. Lett. **95**, 196402 (2005).

[12]H. W. Yeom, J. R. Ahn, H. S. Yoon, I.-W. Lyo, H. Jeong, and S. Jeong, Phys. Rev. B **72**, 035323 (2005).

[13]I. Barke, F. Zheng, T. K. Rügheimer, and F. J. Himpsel, Phys. Rev. Lett. **97**, 226405 (2006).

[14]S. K. Ghose, I. K. Robinson, P. A. Bennett, and F. J. Himpsel, Surf. Sci. **581**, 199 (2005).

[15]W. Voegeli, T. Takayama, K. Kubo, M. Abe, Y. Iwasawa, T. Shirasawa, and T. Takahashi, e-J. Surf. Sci. Nanotechnol. **6**, 281 (2008).

[16]P. C. Snijders, S. Rogge, and H. H. Weitering, Phys. Rev. Lett. **96**, 076801 (2006).

[17]K.-D. Ryang, P. G. Kang, H. W. Yeom, and S. Jeong, Phys. Rev. B **76**, 205325 (2007).

[18]P.-G. Kang, J. S. Shin, and H. W. Yeom, Surf. Sci. **603**, 2588 (2009).

[19]J. N. Crain and D. T. Pierce, Science **307**, 703 (2005).

[20]J. Viernow, J.-L. Lin, D. Y. Petrovykh, F. M. Leibsle, F. K. Men, and F. J. Himpsel, Appl. Phys. Lett. **72**, 948 (1998).

[21]I. Barke, F. Zheng, S. Bockenhauer, K. Sell, V. V. Oeynhausen, K. H. Meiwes-Broer, S. C. Erwin, and F. J. Himpsel, Phys. Rev. B **79**, 155301 (2009).

[22]M. Krawiec, Phys. Rev. B **81**, 115436 (2010).

[23]S. C. Erwin, Phys. Rev. Lett. **91**, 206101 (2003).

[24]S. Riikonen and D. Sánchez-Portal, Phys. Rev. B **77**, 165418 (2008).

[25]D. Sánchez-Portal, S. Riikonen, and R. M. Martin, Phys. Rev. Lett. **93**, 146803 (2004).

[26]S. Riikonen and D. Sánchez-Portal, Phys. Rev. B **76**, 035410 (2007).

[27]See Supplemental Material at http://link.aps.org/supplemental/10.1103/PhysRevB.85.073401 for the time-dependent STM images.

[28]W. P. Su and J. R. Schrieffer, Phys. Rev. Lett. **46**, 738 (1981).